Physics of the Earth and Planetary Interiors 329-330 (2022) 106907

Contents lists available at ScienceDirect

Physics of the Earth and Planetary Interiors

journal homepage: www.elsevier.com/locate/pepi

The effect of water on the outer core transport properties

Yunguo Li [a,b,*], Xuan Guo [a,b,*], Lidunka Vočadlo [c], John P. Brodholt [c,d], Huaiwei Ni [a,b]

[a] CAS Key Laboratory of Crust-Mantle Materials and Environments, School of Earth and Space Sciences, University of Science and Technology of China, Hefei 230026, China
[b] CAS Center for Excellence in Comparative Planetology, School of Earth and Space Sciences, University of Science and Technology of China, Hefei 230026, China
[c] Department of Earth Sciences, University College London, Gower Street, London WC1E 6BT, United Kingdom
[d] Centre for Earth Evolution and Dynamics, University of Oslo, Oslo, Norway

ARTICLE INFO

Keywords:
Viscosity
Diffusion
Outer core
Water

ABSTRACT

Recent studies suggest that incorporation of water in the core during core-mantle differentiation is highly plausible; this could significantly influence outer-core transport properties, which has yet to be rigorously studied. We performed *ab initio* molecular dynamics calculations to investigate the effect of water on the transport properties of liquid iron. We find, at the thermodynamic limit, that the self-diffusion coefficients for Fe are remarkably larger than previously reported values, with and without water. Both the bulk and shear viscosities are of the order of 10^{-3} Pa·s for the outer core. Water, in the form of H or H_2O, can enhance the diffusion of Fe moderately and cause a reduction in both the shear and bulk viscosities, giving rise to an inviscid outer core. The fast liquid Fe dynamics is consistent with the origin and stability of a chemically stratified layer at the topmost outer core. By considering the density jump at the inner-core boundary, we determine that the H content cannot exceed 0.3 wt% in the outer core.

1. Introduction

Transport properties of the outer core, especially viscosity, are fundamental for our understanding of core processes and their geophysical implications (Glatzmaier and Roberts, 1995; Kuang and Bloxham, 1997). Viscosity is a key parameter to model outer core convection and the geodynamo process, and also important for the interpretation of geodetic and seismological data. For example, the shear viscosity coefficient of the outer core is a basic input for dynamo simulations, and the bulk viscosity is responsible for seismic attenuation in the outer core (Anderson, 1980). Both the shear and bulk viscosity are important for the attenuation of longitudinal waves, but only the shear viscosity contributes to the damping of whole Earth torsional mode oscillation and only the bulk viscosity for the damping of radial mode oscillation (Anderson, 1980).

The core is composed of several percent of Ni and also several percent of light elements, most likely to be Si, S, O, C and H (Hirose et al., 2013; Hirose et al., 2021; McDonough and Sun, 1995) and there have been several studies attempting to quantify the effect of light elements on core transport properties. Firstly, the presence of Ni in the core seems to have no effect on viscosity (Zhang and Guo, 2000). The effect of S on the viscosity of the outer core has been extensively studied but with conflicting results. For instance, Dobson et al. (2000) and Pommier et al. (2021) observed an increase of viscosity with increasing S content, while Terasaki et al. (2001) observed an opposite trend. *Ab initio* calculations seem to suggest no strong effect of S on viscosity of Fe (Alfè and Gillan, 1998; Vočadlo et al., 2000). For C, Terasaki et al. (2006) found no difference between the Fe—S and Fe—C eutectic liquids. Pozzo et al. (2013) reported viscosities of two mixtures $Fe_{0.82}Si_{0.1}O_{0.08}$ and $Fe_{0.79}Si_{0.08}O_{0.13}$ along the adiabats and found no difference to pure Fe. Posner and Steinle-Neumann (2019) inferred the viscosity from calculated diffusion coefficients of $Fe_{96}O_4$ *via* the Stokes-Einstein relation and also suggested little influence of O on viscosity; conversely Ichikawa and Tsuchiya (2015) found a monotonical decrease of viscosity with increasing O concentration from 0 to 50 mol%. Nevertheless, those calculations suggest that the O effect on viscosity is only distinguishable when its content is large enough, possibly over 20 mol%. Therefore, the light elements, at just the few percent thought to exist in the core, are unlikely to induce substantial change of the viscosity of liquid iron. However, it is possible that H may bring significant changes to core viscosity since its diffusion in iron is much higher than that of the other light elements. Posner and Steinle-Neumann (2019) inferred the viscosity of $Fe_{96}H_4$

* Corresponding author at: CAS Key Laboratory of Crust-Mantle Materials and Environments, School of Earth and Space Sciences, University of Science and Technology of China, Hefei 230026, China.
E-mail addresses: liyunguo@ustc.edu.cn (Y. Li), guoxuan@ustc.edu.cn (X. Guo).

https://doi.org/10.1016/j.pepi.2022.106907
Received 23 February 2022; Received in revised form 2 June 2022; Accepted 18 June 2022
Available online 22 June 2022

based on the Stokes-Einstein relation and found the viscosity is lowered by almost an order of magnitude compared to pure Fe. However, the applicability of the original Stokes-Einstein equation that relates viscosity to atomic diffusion may not be valid for H, especially when the solute atom size or mass is smaller than that of solvent (Ould-Kaddour and Levesque, 2000).

Water, although mostly seen in the form of H_2O molecule in the hydrosphere, generally refers to the various H-containing species in minerals or melts (Peslier et al., 2017). Recent studies found H could explain the observed core properties (Hirose et al., 2019; Tagawa et al., 2016; Tagawa et al., 2021; Umemoto and Hirose, 2015; Wang et al., 2021). Partition calculations and experiments suggest over four oceans of water could have entered the core (Li et al., 2020; Tagawa et al., 2021; Yuan and Steinle-Neumann, 2020), and such an amount of water together with a few percent Si can perfectly explain the inner-core seismic properties (Wang et al., 2021). It is then interesting to investigate how H influences other core properties. Therefore, in this paper. we performed *ab initio* molecular dynamics simulations to derive the structural and transport properties of water-containing liquid Fe. We calculate self-diffusion coefficients, bulk and shear viscosities of liquid Fe with H/H_2O under core conditions and discuss the geophysical implications for our planet.

2. Methods

The self-diffusion coefficient (D) of a liquid can be calculated *via* the Einstein formula (Frenkel and Smit, 2001)

$$D = \frac{\partial \langle \boldsymbol{r}^2(t) \rangle}{2d \bullet \partial t} \tag{1}$$

where t is the time, $\boldsymbol{r}$ is the displacement, and d is the dimension of the system. The ensemble average $\langle \boldsymbol{r}^2(t) \rangle$ is denoted as the mean squared displacement (MSD), which can be directly retrieved from molecular dynamics trajectories. However, molecular dynamic simulations are always done in limited-size supercells, which are not always large enough to converge the long-range interactions such as the electrostatic and hydrodynamic interactions. Therefore, a size dependence exists for the derivation of D from MD. A simple analytic correction was derived by Yeh and Hummer (2004) based on hydrodynamic arguments

$$\delta D = D^{\infty} - D^{\mathrm{MD}} = \frac{k_B T \xi}{f \pi \eta_s L} \tag{2}$$

where D^{MD} is the one calculated from MD and D^{∞} denotes the diffusion coefficient at the thermodynamic limit. f (= 6 or 4) is a constant determined by the choice of stick or slip hydro-dynamic boundary conditions at the solute surface, k_B is the Boltzmann constant, T is the absolute temperature, $\xi = 2.837297$ is a parameter derived from Ewald type summation, and η_s is the shear viscosity and L is the length of the supercell. Combining the Stokes-Einstein relation

$$D^{\infty} = \frac{k_B T}{f \pi \eta_s R} \tag{3}$$

where R is the hydrodynamic radius of the particle, D^{∞} can also be calculated by

$$D^{\infty} \approx D^{\mathrm{MD}} \times \left(1 - \frac{2R\xi}{3L}\right)^{-1} \tag{4}$$

for the slip boundary condition assumed in the hydrodynamic theory, which applies best to the liquid alloy.

The shear viscosity of liquid can be estimated from the self-diffusion coefficient from the Eyring/Stokes-Einstein. It can also be directly evaluated by the Green-Kubo equation using stress tensors obtained from molecular dynamics (Frenkel and Smit, 2001)

$$\eta_s = \frac{V}{k_B T} \int_0^{\infty} dt \langle P_{\alpha\beta}(t) P_{\alpha\beta}(0) \rangle \tag{5}$$

where V is the cell volume of the simulation, α and β are the Cartesian component, and $P_{\alpha\beta}$ is the off-diagonal element of stress tensor. The integrand is called the stress auto-correlation function. The bulk viscosity from the Green-Kubo relation is calculated by

$$\eta_v = \frac{V}{k_B T} \int_0^{\infty} dt \langle \delta P(t) \delta P(0) \rangle \tag{6}$$

where δP is the instantaneous pressure of the system. There is no clear size dependence for viscosities calculated from MD (Yeh and Hummer, 2004). Therefore, we used a supercell of 100 atoms for liquid Fe. For further explanation for the convergence of the diffusion coefficient and viscosity with respect to the system size, we refer the reader to previous literatures (Celebi et al., 2021; Schoen and Hoheisel, 1985).

Two compositions of water-containing liquid Fe were investigated, which are modelled by using supercells $Fe_{100}H_{10}$ and $Fe_{100}H_{10}O_5$ containing 110 and 115 atoms, respectively. The first composition $Fe_{100}H_{10}$ without oxygen defines a redox state with infinitely small oxygen fugacity, representing an extremely reduced condition. The second composition $Fe_{100}H_{10}O_5$ represents a more oxidized condition. By using these two compositions, we intend to see how the redox state can change the water effect on the core transport properties. We performed AIMD calculations just close to the adiabat curve of pure Fe at 135 GPa and 330 GPa (Pozzo et al., 2013), corresponding to core-mantle boundary (CMB) and inner-core boundary (ICB) conditions. Two temperatures (4500 K and 5000 K) were considered at 135 GPa, and three temperatures (6000 K, 6500 K, 7000 K) were considered at 330 GPa.

AIMD were performed within density functional theory (DFT) level with the projector augmented wave (PAW) method (Kresse and Furthmüller, 1996; Kresse and Hafner, 1993) using the VASP code (Blöchl, 1994; Kresse and Joubert, 1999). Exchange-correlation effects were treated by the generalized gradient approximation (GGA) parameterized by Perdew, Burke and Ernzerhof (Perdew et al., 1996). Fermi–Dirac statistics were used to populate single particle orbitals. A single Gamma point and an energy cutoff of 400 eV were used, which lead to a Pulay stress no larger than 3 GPa. The structures were first relaxed by using constrained NPT calculations to obtain equilibrium volumes under target pressure and temperature. The derived lattice parameters were then used for NVT calculations running over 30 ps for pure Fe and 20 ps for others, which converge diffusion coefficients and viscosities with the uncertainties less than 5%.

3. Results and discussion

3.1. Liquid structure of water-containing Fe

H can be present in various species in minerals or melts, which determine how H influences the properties of iron. We first analyzed the structural features of water-containing liquid Fe and the speciation of H. Fig. 1 shows the radial distribution functions (RDFs) for liquid Fe_{100}, $Fe_{100}H_{10}$ and $Fe_{100}H_{10}O_5$ at 135 GPa, and Fig. 2 shows the RDFs at 330 GPa. At 135 GPa, the characters of RDFs are almost the same for 4500 K and 5000 K except that the peaks are shifted to larger distances for 5000 K, but even the shifts are almost indistinguishable to naked eyes in Fig. 1. Similarly, the RDFs for the three temperatures at 330 GPa also show almost the same characters, as shown in Fig. 2. However, it is evident that the RDFs involving Fe show a first-neighbor-distance peak weakening with the increasing temperature, at both 135 GPa and 330 GPa. Such a feature is general for all systems as a result of increased homogenization and idealization of liquid structure at high temperatures.

At both 135 GPa and 330 GPa, the RDFs of Fe—Fe in Fe_{100} show a typical liquid structure feature with a prominent first-neighbor-distance

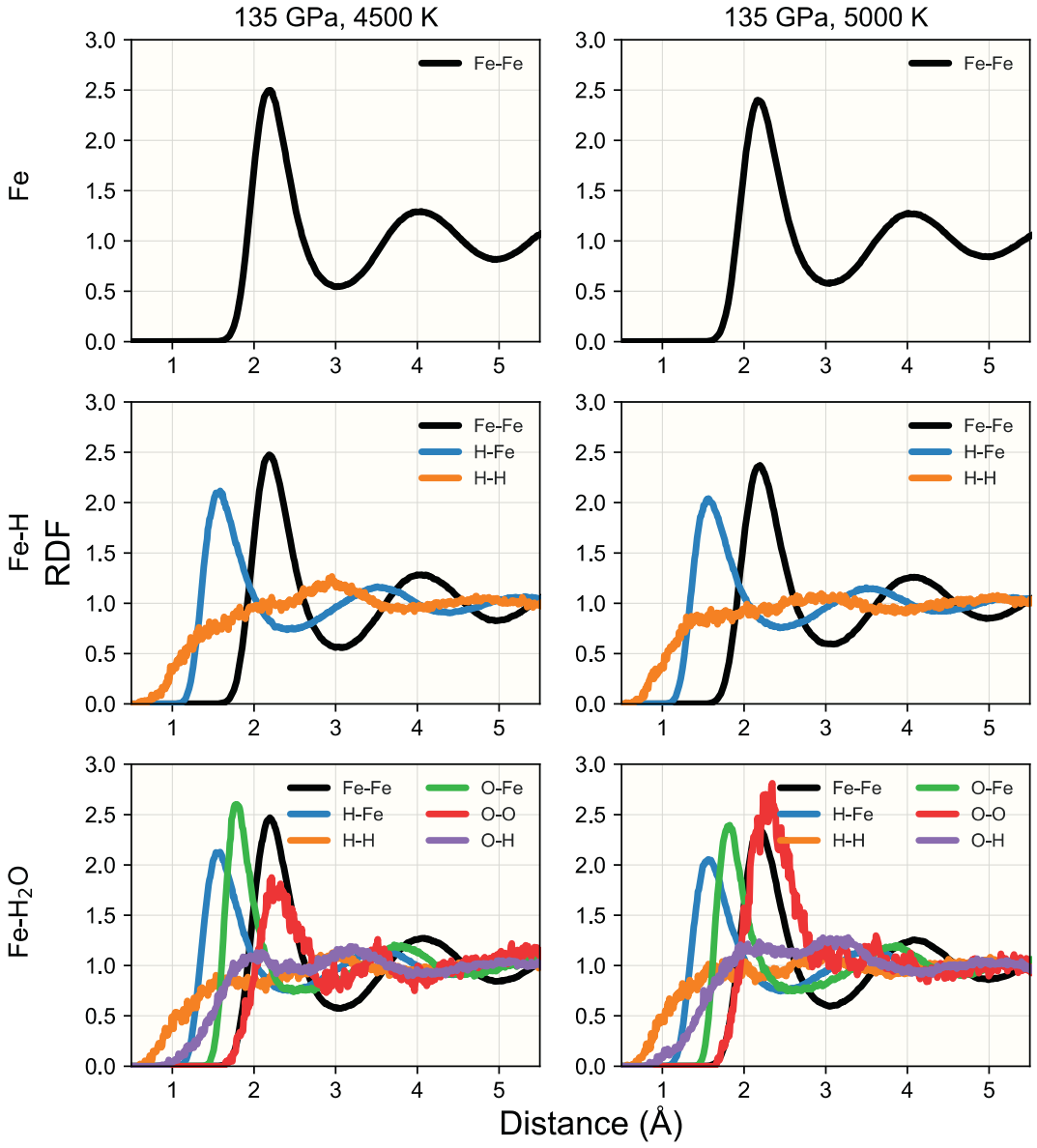

Fig. 1. Radial distribution functions calculated for liquid Fe_{100}, $Fe_{100}H_{10}$ and $Fe_{100}H_{10}O_5$ at 135 GPa.

peak followed by weakening further peaks fluctuating around 1. By integrating the RDF to the distance of its first valley we obtained the coordination number of the first shell, as shown in Fig. 3, which is 13.1 at 135 GPa (4500 K) and 13.3 at 330 GPa (6500 K), with the valley position at 3.01 Å and 2.84 Å, respectively. The coordination numbers are a little bit larger but still similar to that in solid hexagonal-closed-packed (*hcp*) Fe at about the same conditions (Li et al., 2019; Li et al., 2018) (and slightly higher than the low temperature coordination number in closed-packed crystals of 12). At high temperatures this coordination increases as the first- and second-shell atoms mix due to dynamics.

The Fe—Fe bond length and the coordination number in both $Fe_{100}H_{10}$ and $Fe_{100}H_{10}O_5$ as shown in Fig. 3 remain almost the same as the pure liquid, at both 135 and 330 GPa. If H were to take the "close-packing" position in liquid Fe, the coordination number of Fe should decrease in proportion to the molar fraction of H, by 10%. That it is significantly less suggests that the H lies in the "interstitial" sites of closed-packed Fe. In $Fe_{100}H_{10}O_5$, the coordination of Fe shows a decrease of ~4.6%, which is almost the same as the molar fraction of O (4.8% if we ignore H which lies in interstitial positions). Either O is mostly in the "close-packing" position or the presence of O in the "interstitial" position hampers the mixing of the second shell with the first shell of Fe atoms. Considering the large volume difference between Fe and O atoms, it is unlikely that O will be in the "close-packing" position (Li et al., 2019). The second-shell bond length of Fe—Fe is twice as large as the O—Fe bond length, meaning that O can be comfortably accommodated in the "interstitial" position and its presence will hamper the mixing of second-shell Fe atoms into the first shell. Given the coordination number of O, the "interstitial" site would be equivalent to the octahedral center in the solid *hcp* Fe. There is an evident increase of coordination for O but not for H from 135 GPa to 330 GPa as shown in Fig. 3. This is also related to the atom size that O is larger than H and likely more affected by pressure.

H has no bonding to H and O in $Fe_{100}H_{10}$ and $Fe_{100}H_{10}O_5$. The H—H and H—O RDFs show almost a flat feature, meaning the chance is equal for H to find another H or O atom at any distance beyond a minimum. H exists in an almost free and ideal manner in liquid Fe under core conditions regardless of oxygen fugacity. There is an evident O—O RDF peak shown in Figs. 1 and 2, and the integration of the RDF leads to a coordination number close to 1, which is ~5% of the total coordination

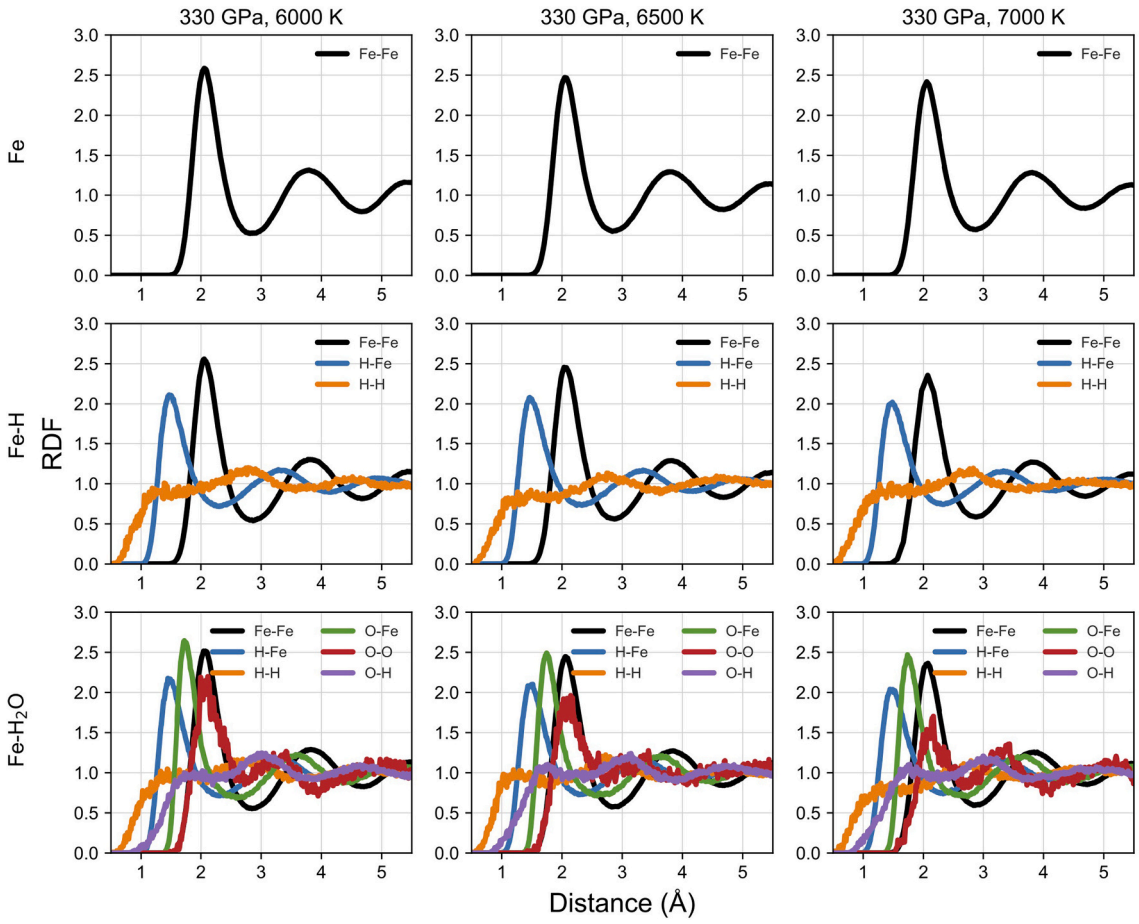

Fig. 2. Radial distribution functions calculated for liquid Fe_{100}, $Fe_{100}H_{10}$ and $Fe_{100}H_{10}O_5$ at 330 GPa.

of O. Such a percentage is close to the molar fraction of O (here the molar fraction would be defined by the number of O atoms divided by the numbers of O atoms and "octahedral" site), and this suggests that there is no preference of O—O bonding in liquid Fe. Overall, both H and O show an almost ideal state in liquid Fe under core conditions. This is consistent with previous findings that water behaves more ideal with the increasing temperature and pressure (Soubiran and Militzer, 2015).

3.2. Diffusion coefficients

Fig. 4 shows the MSDs for Fe, H and O as a function of simulation time. MSDs from the initial MD steps show a different slope due to thermal motion, and only after a while with enough collisions the diffusive regime could be reached. The initial steps were dropped when fitting MSDs with the Einstein relation to obtain the self-diffusion coefficients D_{Fe}^{MD}s, and the results are shown in Table 1. D_{Fe}^{MD} is 5.03×10^{-9} m^2/s and 5.79×10^{-9} m^2/s at 135 GPa and 330 GPa, respectively, and they are roughly consistent with previous findings at core conditions (Huang et al., 2019; Ichikawa and Tsuchiya, 2015; Li et al., 2021; Pozzo et al., 2013). However, the size dependence of D_{Fe}^{MD} is already obvious by looking at previous studies. Using a supercell of 80 atoms, Ichikawa and Tsuchiya (2015) obtained $D_{Fe}^{MD} \approx 4.4 \times 10^{-9}$ m^2/s at 136 GPa and 4581 K. Posner and Steinle-Neumann (2019) used a supercell of 150 atoms, and $D_{Fe}^{MD} \approx 5.37 \times 10^{-9}$ m^2/s at 135 GPa and 4500 K from extrapolation of their data. Our D_{Fe}^{MD} calculated in a supercell of 100 atoms lies between those two values. We have corrected the MD derived self-diffusion coefficients to the thermodynamic limit, which are listed in Table 2. However, as can be seen in Table 1, at the thermodynamic limit D_{Fe}^{∞} is 6.42×10^{-9} m^2/s at 135 GPa and 4500 K, which is 46% larger than the reported data from Ichikawa and Tsuchiya (2015).

As shown in Table 2, our results show that water has a moderate effect on Fe diffusivity. At 135 GPa and 4500 K, D_{Fe}^{∞} increases by 11% and 21% in $Fe_{100}H_{10}$ and $Fe_{100}H_{10}O_5$ respectively; at 330 GPa and 6500 K, D_{Fe}^{∞} increases by 4% and 19% in $Fe_{100}H_{10}$ and $Fe_{100}H_{10}O_5$, respectively. H increases the Fe diffusivity more effectively at 135 GPa and 4500 K than at 330 GPa, but O seems to be more effective in increasing the Fe diffusivity at 330 GPa. Given that D_O is much higher than in the Fe—O binary at 135 GPa (Pozzo 2013), H seems to have a positive effect on O diffusion. H diffuses fast in liquid Fe, at a speed about 11 times larger than that of pure Fe at both 135 and 330 GPa. O diffuses at a rate twice that of Fe at 135 and 330 GPa. Graham's law states that the rate of diffusion is inversely proportional to the square root of the ratio of molecular mass, accordingly H and O should be 7.44 and 1.87 times faster than Fe. For both H and O, their diffusion coefficients are always higher than the Graham's law prediction. Such a phenomena can be attributed to the atom size and the blocking effect: the small-volume atoms have more accessible spare space or voids that allow them to diffuse but block the large-volume atoms.

3.3. Viscosities

Outer core viscosity was estimated to be $10^{8\sim9}$ Pa · s from p-wave attenuation and $10^{-2\sim9}$ Pa · s from analysis of the radial and torsional modes of free oscillation (Secco, 1995), which are significantly larger than those from mineral physics studies. Experimental measurement of liquid iron viscosity under high pressure is typically based on the Stokes's viscometry method, which involves measuring the velocity of a probe sphere that moves through a pressurized melt. Initial measurements were limited to 7 GPa and subjected to large uncertainties due to experimental challenges, giving the shear viscosity ranging from 10^{-2}

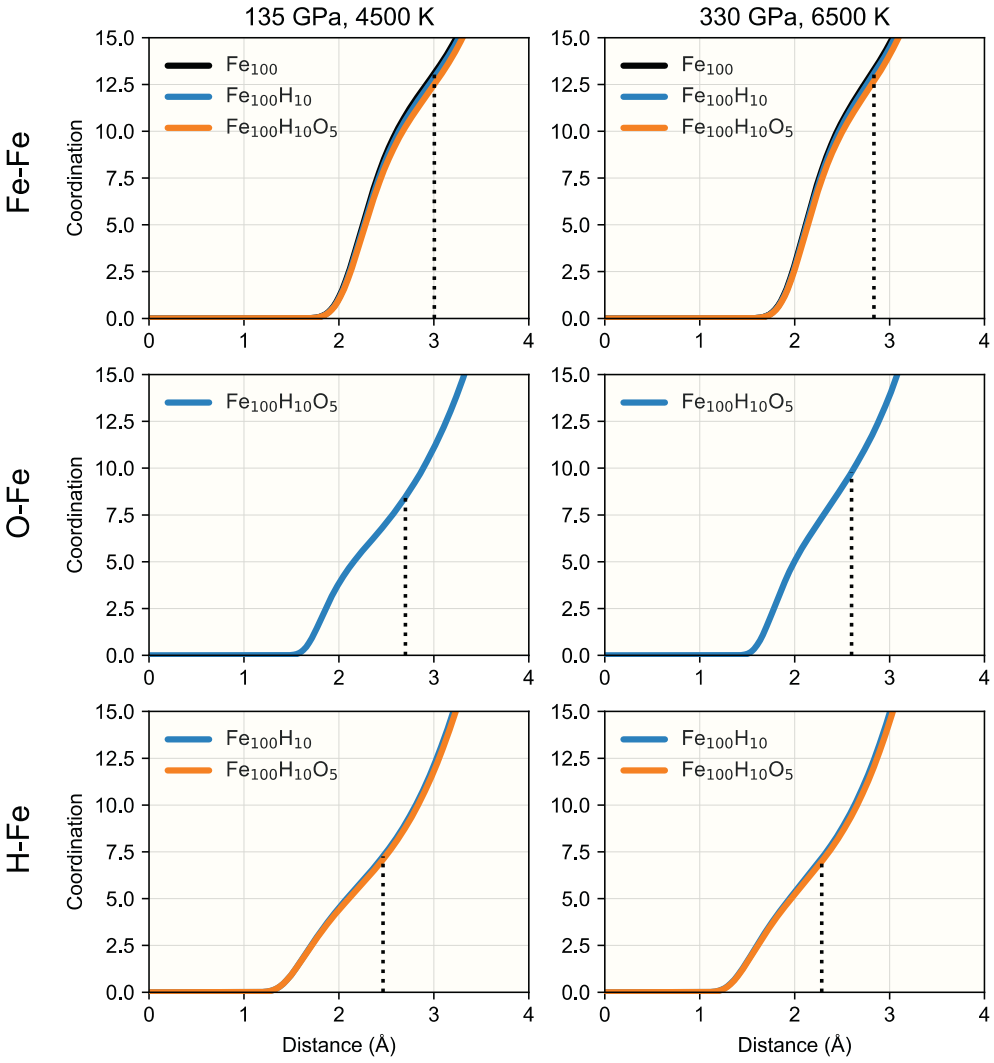

Fig. 3. The number of Fe atoms coordinated to Fe, O and H. The vertical dotted line indicates the position of the first valley in the corresponding RDF.

Pa · s to 10^4 Pa · s (Brazhkin, 1998; LeBlanc and Secco, 1996; Secco et al., 1998). With the improvement of experimental techniques, estimates converged to 10^{-2} Pa · s (Dobson et al., 2000; Pommier et al., 2021; Rutter et al., 2002; Terasaki et al., 2001; Terasaki et al., 2006; Urakawa et al., 2001). It was found that the shear viscosity is constant along the pressure dependent melting boundary (Rutter et al., 2002), which allows for a direct estimation of outer-core viscosity from experiments at low pressures. The experimental findings are supported by *ab initio* calculations that also suggest an outer-core shear viscosity around 10^{-2} Pa · s (de Wijs et al., 1998; Ichikawa and Tsuchiya, 2015; Li et al., 2021; Vočadlo et al., 2000). Experimental or theoretical studies on bulk viscosity are rare and we only note one calculation by Zhang et al. (2000) using empirical molecular dynamics. They found outer-core viscosity to be of the order of $10^{-3\sim-4}$ Pa · s, much lower than previous estimates.

Our calculated viscosities are shown in Fig. 5 as a function of simulation time and also tabulated in Table 2. Viscosities calculated in this way quickly approach the converged values after ~10 ps for pure Fe and ~ 5 ps for the alloys, except for pure Fe at low temperatures. The slow convergence and large fluctuation at low temperatures are possibly because the temperatures are already close to the freezing points. We estimate the viscosity and associated uncertainties using only the results after these equilibration times. The calculated shear viscosities of liquid Fe at both pressures are in agreement with previous theoretical studies (de Wijs et al., 1998; Ichikawa and Tsuchiya, 2015; Vočadlo et al., 2000), supporting an inviscid core. The calculated bulk viscosity is 1.5 − 1.7 mPa · s at 135 GPa and 1.1 − 1.3 mPa · s at 330 GPa, which verify those calculated from the Sutton-Chen potential by Zhang et al. (2000).

The shear viscosity of pure Fe drops significantly from 6000 K to 6500 at 330 GPa, but the further drop from 6500 K to 7000 K is much smaller. The shear viscosity of pure Fe at 135 GPa also does not change much from 4500 K to 5000 K. This indicates that the temperature effect is weakened at high temperatures. Compared to pure Fe, the shear viscosity drops substantially in both $Fe_{100}H_{10}$ and $Fe_{100}H_{10}O_5$ at both pressures. Such a reduction in shear viscosity can be expected from the increase of diffusivity as shown above. The shear viscosity is similar for $Fe_{100}H_{10}$ and $Fe_{100}H_{10}O_5$, possibly because viscosity is already very low with the addition of H. The bulk viscosities of Fe_{100}, $Fe_{100}H_{10}$ and $Fe_{100}H_{10}O_5$ are very low and close to each other, and the effect of water is much weaker than for the shear viscosity. Besides, these similarities also suggest that the water effect on core transport properties is not sensitive to oxygen fugacity.

We also calculated the shear viscosity using the Stokes-Einstein relation and compared them to those from the Green-Kubo equation. We used the averaged self-diffusion coefficients ($D_{avg} = \sum_{i=Fe,H,O}^{i} x_i \bullet D_i$) and averaged atom radius ($R_{avg} = \sum_{i=Fe,H,O}^{i} x_i \bullet R_i$) in the Stokes-Einstein relation. As shown in Fig. 6, the match between the Stokes-Einstein and Green-Kubo calculations is not very good, although they qualitatively agree. If only D_{Fe} and R_{Fe} are used, the Stokes-Einstein at most times

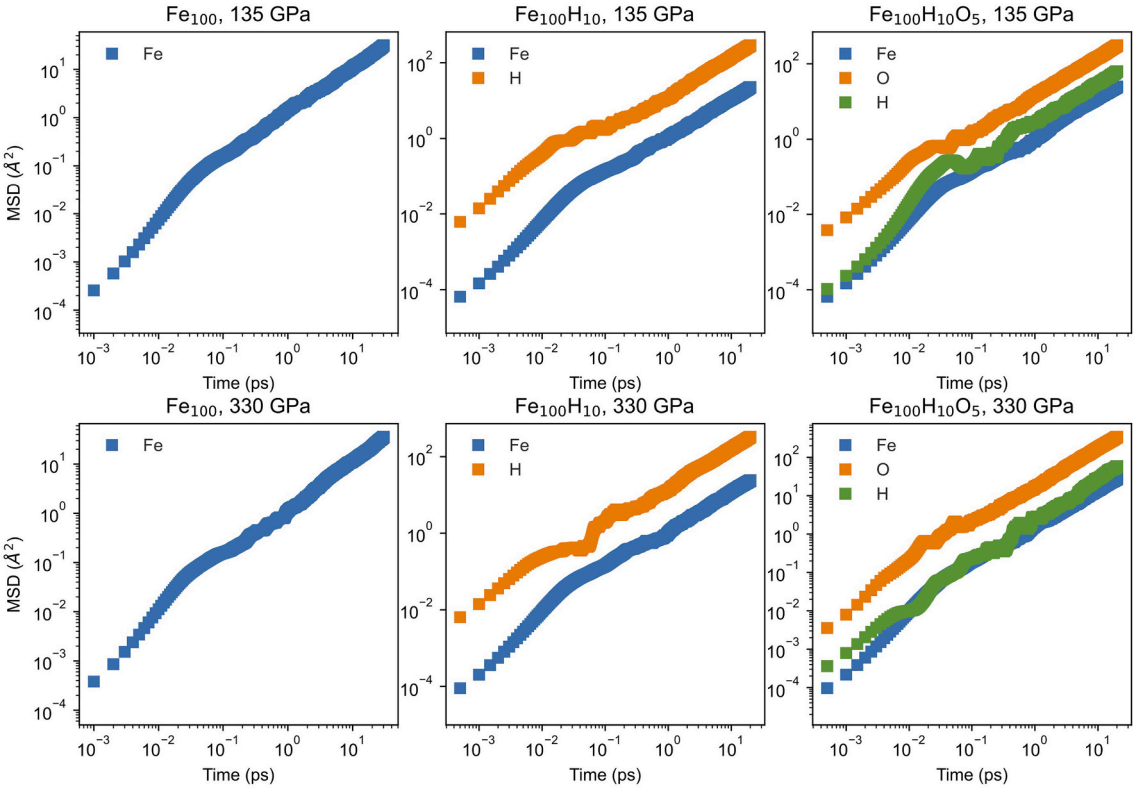

Fig. 4. Mean squared displacements (MSDs) as a function of simulation time at 135 GPa (4500 K) and 330 GPa (6500 K). Diffusion coefficients were fitted from the Einstein formula in the linear region in the plots without the initial steps.

Table 1
Calculated Fe diffusion coefficients in comparison with literature results at similar conditions. Data in bracket correspond to D_{Fe}^{∞} at the thermodynamic limit.

D_{Fe} (10^{-9} m^2/s)	P (GPa)	T (K)	Composition	Source
5.0	328	6350	Fe	Pozzo et al., 2013
5.8	135	4700	Fe	Pozzo et al., 2013
5.0	134	4300	$Fe_{86}Si_{11}O_{11}$	Huang et al., 2019
7.0	134	4800	$Fe_{86}Si_{11}O_{11}$	Huang et al., 2019
4.4	136	4581	Fe	Ichikawa and Tsuchiya, 2015
7.2	135	5000	Fe	Li et al., 2021
5.37	135	4500	Fe	Posner and Steinle-Neumann, 2019
5.03 (6.42)	135	4500	Fe	This study
8.85 (6.93)	135	5000	Fe	This study
5.79 (7.41)	330	6500	Fe	This study

predicts higher viscosities. If the averaged diffusion coefficients D_{avg} are used, the Stokes-Einstein predicts lower viscosities. This is because H and O have much larger diffusion coefficients but their specific contribution to the viscosity is much lower than Fe, which is a problem already known as another size effect in hydrodynamic relations (Ould-Kaddour and Levesque, 2000).

Although the Stokes-Einstein relation does not rigorously hold, the predicted viscosities from diffusion coefficients are very close to the calculated ones. All the light elements diffuse faster than Fe (Posner and Steinle-Neumann, 2019), so the core viscosity is likely to be at the order of 10^{-3} Pa · s or even lower with the presence of water (Li et al., 2020; Tagawa et al., 2021; Yuan and Steinle-Neumann, 2020) and other light elements. This contradicts with the seismic analyses that give the core viscosities of $10^{-2\sim9}$ Pa · s. The large estimates of viscosities from seismic analyses could be due to the large uncertainties introduced during long observation times or the presence of other loss mechanisms.

3.4. Geophysical implications

The H content in our chosen compositions is equivalent to 22 oceans of water in the core, which is higher than that needed to explain inner-core properties but less than that required to explain the outer-core properties if H is the only light element (unlikely) in the core (Umemoto and Hirose, 2015; Wang et al., 2021). Both H and O behave in a way similar or close to the ideal state in liquid Fe under core conditions, and it has been shown that the shear viscosity of liquid Fe—O is linearly dependent on O content (Ichikawa and Tsuchiya, 2015), so we can expect a monotonic change for core properties with the increasing H/H_2O content.

As shown above, the presence of water in the core can moderately enhance the transport properties of the outer core, with increased diffusion coefficients for all elements and reduced viscosities. The low viscosity of liquid Fe and the further reduction by water, immediately indicates an inviscid outer core. This suggests small-scale turbulent circulation would be dominant in core convection, as already proposed by de Wijs et al. (1998). It has been suggested that barodiffusion would accumulate light elements, especially O, at the top of the core over time, (Gubbins and Davies, 2013). The thickness of this layer was estimated to be ~100 km or smaller (Gubbins and Davies, 2013; Ichikawa and Tsuchiya, 2015), which is less than the seismic observations of a stratified layer E' at the top of the outer core (140– 300 km) (Buffett, 2014; Helffrich and Kaneshima, 2010). However, the diffusion coefficients used in the models without corrections to the thermodynamic limit are significantly smaller than (almost half of) ours (Gubbins and Davies, 2013). Since the thickness is proportional to the square root of D_O, using our diffusion coefficients would predict a thickness of ~140 km, consistent with the thickness of the low-velocity layer E'. It has been argued that barodiffusion and an O enriched layer cannot explain the low-velocity layer E' as simply increasing O concentration leads to higher velocities (Brodholt and Badro, 2017), however, the origin and

Table 2
Calculated diffusion coefficients and viscosities at corresponding pressure and temperature conditions. The uncertainties are all less than 5%.

P (GPa)	T (K)	Structure	ρ (g/cm^3)	Element	D^{∞} (10^{-9} m^2/s)	D^{MD} (10^{-9} m^2/s)	η_s (mPa·s)	η_v (mPa·s)
135	4500	Fe_{100}	10.862	Fe	6.42	5.03	6.4	1.5
		$Fe_{100}H_{10}$	10.647	Fe	7.09	5.57	5.1	1.5
				H	79.5	72.0		
		$Fe_{100}H_{10}O_5$	10.472	Fe	7.79	6.11	5.1	1.4
				O	17.9	15.4		
				H	82.9	75.5		
	5000	Fe_{100}	10.764	Fe	8.85	6.93	6.8	1.7
		$Fe_{100}H_{10}$	10.554	Fe	9.28	7.28	5.4	1.4
				H	93.2	84.5		
		$Fe_{100}H_{10}O_5$	10.389	Fe	10.0	7.86	4.7	1.3
				O	23.2	20.0		
				H	98.5	89.6		
330	6000	Fe_{100}	13.190	Fe	5.68	4.44	15.2	1.3
		$Fe_{100}H_{10}$	12.953	Fe	6.45	5.05	8.9	1.3
				H	76.6	69.6		
		$Fe_{100}H_{10}O_5$	12.759	Fe	7.02	5.50	8.1	1.3
				O	15.4	13.2		
				H	78.5	71.4		
	6500	Fe_{100}	13.128	Fe	7.41	5.79	9.6	1.2
		$Fe_{100}H_{10}$	12.902	Fe	7.72	6.04	7.7	1.2
				H	90.0	81.8		
		$Fe_{100}H_{10}O_5$	12.695	Fe	8.85	6.93	7.7	1.2
				O	17.4	14.9		
				H	93.3	84.9		
	7000	Fe_{100}	13.060	Fe	8.69	6.79	8.0	1.1
		$Fe_{100}H_{10}$	12.827	Fe	10.2	7.98	7.4	1.2
				H	106	96.1		
		$Fe_{100}H_{10}O_5$	12.636	Fe	10.7	8.35	8.0	1.3
				O	19.1	16.4		
				H	110	100		

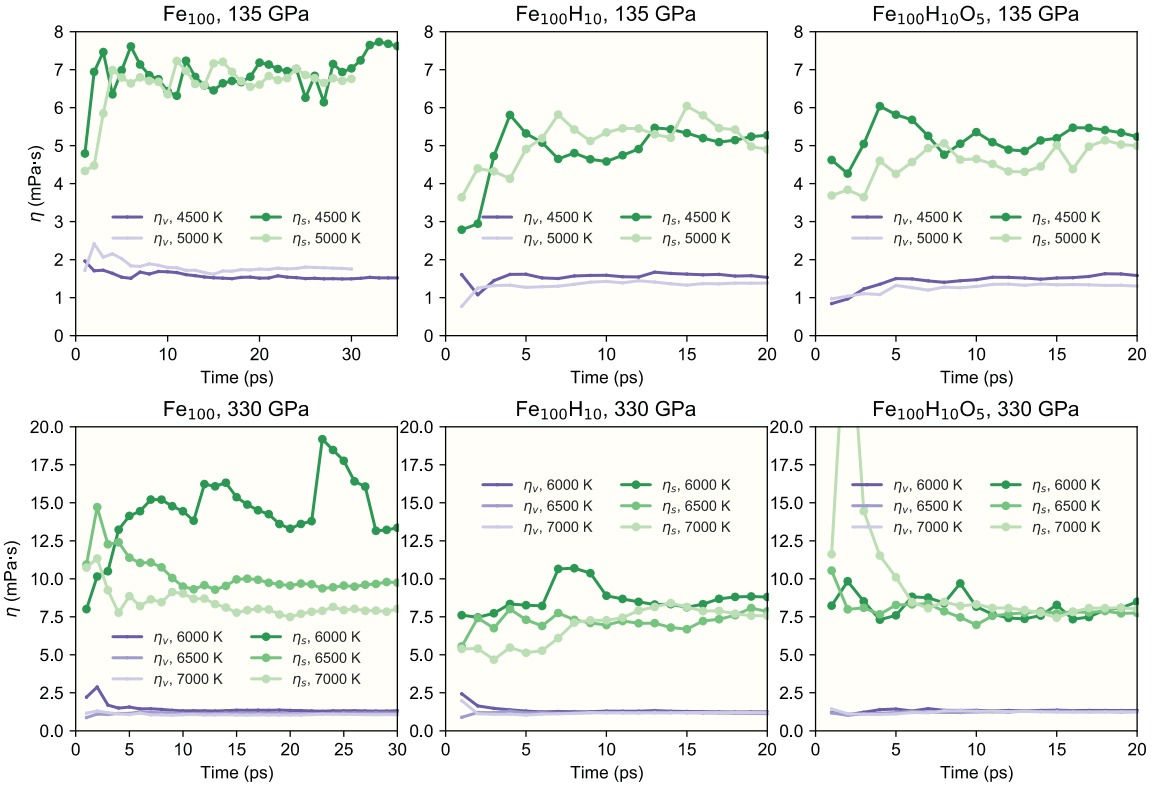

Fig. 5. Shear and bulk viscosities calculated as a function of simulation time at 135 GPa, 4500 K and 330 GPa, 6500 K. The filled squares represent the values calculated at an interval of 1 *ps*.

stability of any layer in the E' layer must consider the faster diffusion coefficients.

Using the densities calculated in this study, we can further constrain the H budget in the core considering the ICB density jump. We use the volume of H in the solid in Wang et al. (2021) that used same methods to this study (hence the volume can be directly compared to the calculated

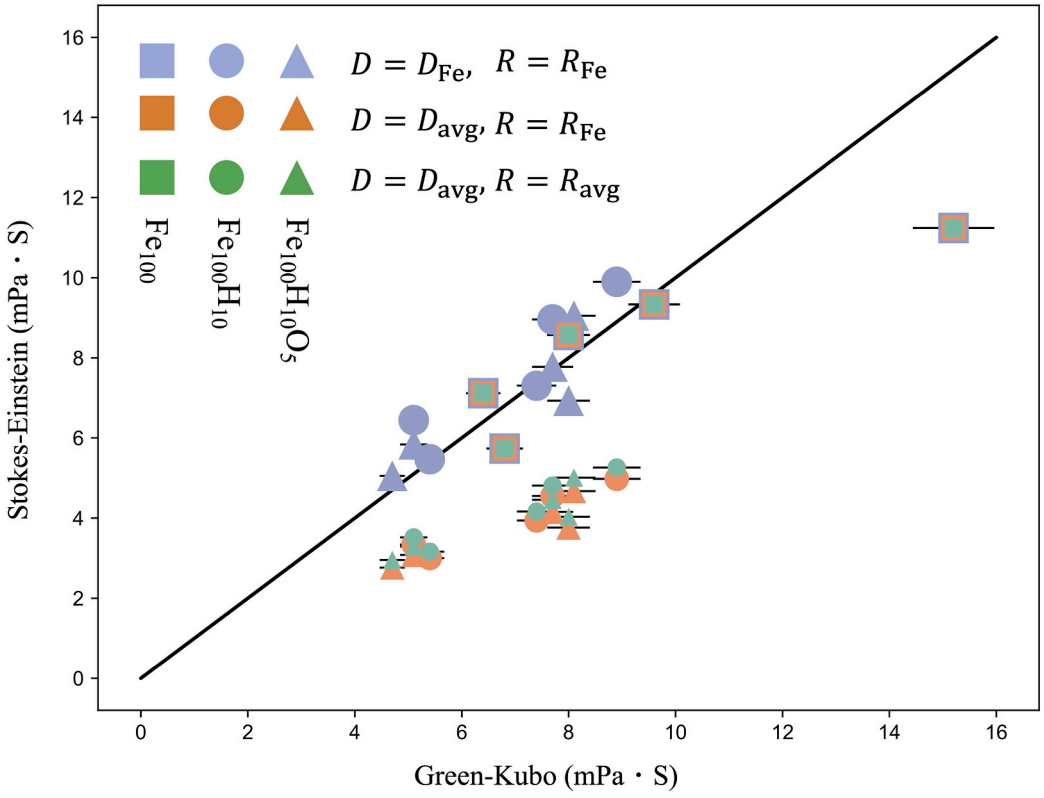

Fig. 6. Shear viscosities calculated from Green-Kubo method *vs.* those from Stokes-Einstein relation. The linear line is for guiding. Three combinations of diffusion coefficient and atom radius were used in Stokes-Einstein relation. D_{Fe} and R_{Fe} refer to the diffusion coefficient and atom radius of Fe, respectively. $D_{avg} = \sum_{i=Fe,H,O}^{i} x_i \bullet D_i$ and $R_{avg} = \sum_{i=Fe,H,O}^{i} x_i \bullet R_i$ are the averaged diffusion coefficient and atom radius, where D_i and R_i are the diffusion coefficient and atom radius for each element in the system. (For interpretation of the references to colour in this figure legend, the reader is referred to the web version of this article.)

H volume in liquid and used for further calculations). H is likely to partition almost equally in the core, but O is known to only exist in the outer core (Alfè et al., 2000). Therefore, we can calculate the densities of Fe for both the solid and liquid in the presence of H or H_2O in the core. Fig. 7 shows the density jump between the solid and liquid as a function of $x_H/(x_H + x_{Fe})$. In the context of weight percentage, if H is the only light element in the core, H content in the whole core cannot exceed 0.3 wt%, equivalent to 35 oceans in the core. If H exists stoichiometrically in the outer core as H_2O, H content in the whole core cannot exceed 0.12 wt%, equivalent to 22 oceans. Therefore, the upper limit of H budget in the core can be significantly reduced from 1 wt% to 0.3 wt% (Umemoto and Hirose, 2015).

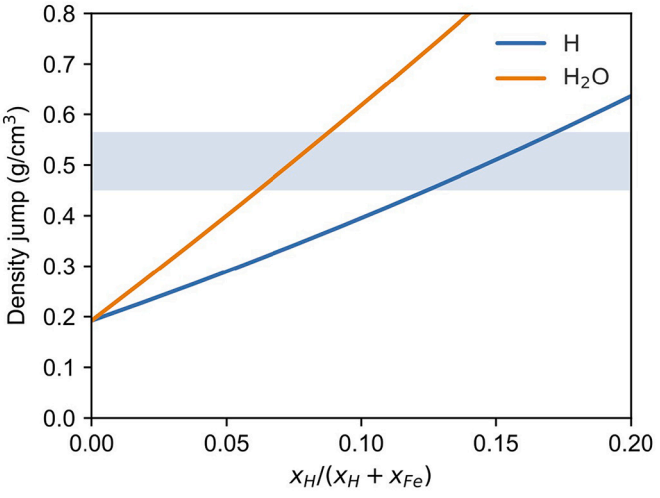

Fig. 7. Density difference at 330 GPa and 6500 K between the solid and liquid as a function of $x_H/(x_H + x_{Fe})$. Shaded region indicates the ICB density jump. The blue and orange lines indicate the density difference for H and H_2O containing core, respectively. (For interpretation of the references to colour in this figure legend, the reader is referred to the web version of this article.)

It is known that the PBE functional used in this study overestimates the volume compared to experiments, so the pressure from PBE should be shifted downward by ~8 GPa at ICB condition (Badro et al., 2014). By extrapolating the volume of H calculated at 135 GPa and 330 GPa, we obtain that the H volume is overestimated by 1.4% at 330 GPa. However, PBE also overestimates the volume of solid Fe at the similar level as for liquid Fe (Pamato et al., 2020; Sun et al., 2018). Thus, most of the error of H volume due to using the PBE functional is cancelled out and negligible. Another source of error for H volume comes from the uncertainty of pressure, which is ~0.07 GPa and propagates to an error of 0.5% on H volume. So, the error for the calculated H volume and density is no more than 1.9%.

4. Conclusions

We have studied the effects of water in liquid Fe at core conditions by using AIMD simulations. We find both H and O atoms exist in liquid Fe in a manner similar or close to the ideal state, and they travel through the "interstitial" positions in liquid Fe at a speed several times of Fe. We show that the correction to the thermodynamic limit is necessary for an accurate determination of self-diffusivity, and the prediction of viscosity from the Stokes-Einstein relation is not reliable. Water in the outer core can effectively enhance the diffusivity and reduce the viscosity. We confirm that the core is an inviscid liquid and should be dominated by small-scale circulation. We further constrain that the content of H in the core cannot exceed 0.3 wt% considering the ICB density jump.

CRediT authorship contribution statement

Yunguo Li: Conceptualization, Methodology, Investigation, Writing – original draft. **Xuan Guo:** Conceptualization, Investigation, Writing – original draft. **Lidunka Vočadlo:** Validation, Writing – review &

editing, Supervision. **John P. Brodholt:** Validation, Writing – review & editing, Supervision. **Huaiwei Ni:** Conceptualization, Writing – review & editing, Supervision.

Declaration of Competing Interest

The authors declare that they have no known competing financial interests or personal relationships that could have appeared to influence the work reported in this paper.

Acknowledgments

We acknowledge the support of National Natural Science Foundation of China (Grants No. 42173040). Y.L. also thanks the support from CAS Hundred Talents Program. The numerical calculations in this paper have been done on the supercomputing system in the Supercomputing Center of University of Science and Technology of China.

References

Alfè, D., Gillan, M.J., 1998. First-principles calculation of transport coefficients. Phys. Rev. Lett. 81 (23), 5161–5164.
Alfè, D., Gillan, M.J., Price, G.D., 2000. Constraints on the composition of the Earth's core from ab initio calculations. Nature 405 (6783), 172–175.
Anderson, D.L., 1980. Bulk attenuation in the earth and viscosity of the core. Nature 285 (5762), 204–207.
Badro, J., Côté, A.S., Brodholt, J.P., 2014. A seismologically consistent compositional model of Earth's core. Proc. Natl. Acad. Sci. 111 (21), 7542–7545.
Blöchl, P.E., 1994. Projector augmented-wave method. Phys. Rev. B 50 (24), 17953.
Brazhkin, V., 1998. Investigation of the crystallization of liquid iron under pressure: extrapolation of the melt viscosity into the megabar range. J. Exp. Theor. Phys. Lett. 68 (6), 502–508.
Brodholt, J., Badro, J., 2017. Composition of the low seismic velocity E′ layer at the top of Earth's core. Geophys. Res. Lett. 44 (16), 8303–8310.
Buffett, B., 2014. Geomagnetic fluctuations reveal stable stratification at the top of the Earth's core. Nature 507 (7493), 484–487.
Celebi, A.T., Jamali, S.H., Bardow, A., Vlugt, T.J.H., Moultos, O.A., 2021. Finite-size effects of diffusion coefficients computed from molecular dynamics: a review of what we have learned so far. Mol. Simul. 47 (10−11), 831–845.
de Wijs, G.A., Kresse, G., Vočadlo, L., Dobson, D., Alfè, D., Gillan, M.J., Price, G.D., 1998. The viscosity of liquid iron at the physical conditions of the Earth's core. Nature 392 (6678), 805–807.
Dobson, D.P., Crichton, W.A., Vočadlo, L., Jones, A.P., Wang, Y., Uchida, T., Rivers, M., Sutton, S., Brodholt, J.P., 2000. In situ measurement of viscosity of liquids in the Fe-FeS system at high pressures and temperatures. Am. Mineral. 85 (11−12), 1838–1842.
Frenkel, D., Smit, B., 2001. Understanding Molecular Simulation: From Algorithms to Applications, Vol. 1. Elsevier.
Glatzmaier, G.A., Roberts, P.H., 1995. A three-dimensional convective dynamo solution with rotating and finitely conducting inner core and mantle. Phys. Earth Planet. Inter. 91 (1), 63–75.
Gubbins, D., Davies, C.J., 2013. The stratified layer at the core–mantle boundary caused by barodiffusion of oxygen, sulphur and silicon. Phys. Earth Planet. Inter. 215, 21–28.
Helffrich, G., Kaneshima, S., 2010. Outer-core compositional stratification from observed core wave speed profiles. Nature 468 (7325), 807–810.
Hirose, K., Labrosse, S., Hernlund, J., 2013. Composition and state of the core. Annu. Rev. Earth Planet. Sci. 41 (1), 657–691.
Hirose, K., Tagawa, S., Kuwayama, Y., Sinmyo, R., Morard, G., Ohishi, Y., Genda, H., 2019. Hydrogen Limits Carbon in Liquid Iron. Geophys. Res. Lett. 46 (10), 5190–5197.
Hirose, K., Wood, B., Vočadlo, L., 2021. Light elements in the Earth's core. Nat. Rev. Earth Environ. 2 (9), 645–658.
Huang, D., Badro, J., Brodholt, J., Li, Y., 2019. Ab initio molecular dynamics investigation of molten Fe–Si–O in Earth's core. Geophys. Res. Lett. 46 (12), 6397–6405.
Ichikawa, H., Tsuchiya, T., 2015. Atomic transport property of Fe–O liquid alloys in the Earth's outer core P, T condition. Phys. Earth Planet. Inter. 247, 27–35.
Kresse, G., Furthmüller, J., 1996. Efficiency of ab-initio total energy calculations for metals and semiconductors using a plane-wave basis set. Comput. Mater. Sci. 6 (1), 15–50.
Kresse, G., Hafner, J., 1993. *Ab initio* molecular dynamics for open-shell transition metals. Phys. Rev. B 48 (17), 13115.
Kresse, G., Joubert, D., 1999. From ultrasoft pseudopotentials to the projector augmented-wave method. Phys. Rev. B 59 (3), 1758.
Kuang, W., Bloxham, J., 1997. An Earth-like numerical dynamo model. Nature 389 (6649), 371–374.
LeBlanc, G.E., Secco, R.A., 1996. Viscosity of an Fe-S liquid up to 1300°C and 5 GPa. Geophys. Res. Lett. 23 (3), 213–216.
Li, Y., Vočadlo, L., Brodholt, J., 2018. The elastic properties of *hcp*-Fe alloys under the conditions of the Earth's inner core. Earth Planet. Sci. Lett. 493, 118–127.
Li, Y., Vočadlo, L., Alfè, D., Brodholt, J., 2019. Carbon partitioning between the Earth's inner and outer Core. J. Geophys. Res. Solid Earth 124 (12), 12812–12824.
Li, Y., Vočadlo, L., Sun, T., Brodholt, J.P., 2020. The Earth's core as a reservoir of water. Nat. Geosci. 13 (6), 453–458.
Li, Q., Sun, T., Zhang, Y., Xian, J., Vočadlo, L., 2021. Atomic transport properties of liquid Iron at conditions of planetary cores. J. Chem. Phys. 155, 194505.
McDonough, W.F., Sun, S.S., 1995. The composition of the earth. Chem. Geol. 120 (3), 223–253.
Ould-Kaddour, F., Levesque, D., 2000. Molecular-dynamics investigation of tracer diffusion in a simple liquid: test of the stokes-Einstein law. Phys. Rev. E 63 (1), 011205.
Pamato, M.G., Li, Y., Antonangeli, D., Miozzi, F., Morard, G., Wood, I.G., Vočadlo, L., Brodholt, J.P., Mezouar, M., 2020. Equation of state of hcp Fe-C-Si alloys and the effect of C incorporation mechanism on the density of hcp Fe alloys at 300 K. J. Geophys. Res. Solid Earth 125 (12), e2020JB020159.
Perdew, J.P., Burke, K., Ernzerhof, M., 1996. Generalized gradient approximation made simple. Phys. Rev. Lett. 77 (18), 3865–3868.
Peslier, A.H., Schönbächler, M., Busemann, H., Karato, S.-I., 2017. Water in the Earth's interior: distribution and origin. Space Sci. Rev. 212 (1–2), 743–810.
Pommier, A., Leinenweber, K., Pirotte, H., Yu, T., Wang, Y., 2021. In situ electrical resistivity and viscosity measurements of iron alloys under pressure using synchrotron X-ray radiography. High Pressure Res. 41 (1), 1–13.
Posner, E.S., Steinle-Neumann, G., 2019. Mass transport and structural properties of binary liquid iron alloys at high pressure. Geochem. Geophys. Geosyst. 20 (7), 3556–3568.
Pozzo, M., Davies, C., Gubbins, D., Alfè, D., 2013. Transport properties for liquid silicon-oxygen-iron mixtures at Earth's core conditions. Phys. Rev. B 87 (1), 014110.
Rutter, M.D., Secco, R.A., Liu, H., Uchida, T., Rivers, M.L., Sutton, S.R., Wang, Y., 2002. Viscosity of liquid Fe at high pressure. Phys. Rev. B 66 (6), 060102.
Schoen, M., Hoheisel, C., 1985. The shear viscosity of a Lennard-Jones fluid calculated by equilibrium molecular dynamics. Mol. Phys. 56 (3), 653–672.
Secco, R.A., 1995. Mineral Physics & Crystallography: A Handbook of Physical Constants, Vol. 2. American Geophysical Union.
Secco, R., LeBlanc, G., Yang, H., Seibel, J., 1998. High pressure viscosity of an Fe-S liquid: experimentally derived estimate of the viscosity of Earth's outer core. In: Washington DC American Geophysical Union Geophysical Monograph Series, 101, pp. 495–505.
Soubiran, F., Militzer, B., 2015. Hydrogen–water mixtures in giant planet interiors studied with ab initio simulations. High Energy Density Phys. 17, 157–161.
Sun, T., Brodholt, J.P., Li, Y., Vočadlo, L., 2018. Melting properties from ab initio free energy calculations: Iron at the Earth's inner-core boundary. Phys. Rev. B 98 (22), 224301.
Tagawa, S., Ohta, K., Hirose, K., Kato, C., Ohishi, Y., 2016. Compression of Fe–Si–H alloys to core pressures. Geophys. Res. Lett. 43 (8), 3686–3692.
Tagawa, S., Sakamoto, N., Hirose, K., Yokoo, S., Hernlund, J., Ohishi, Y., Yurimoto, H., 2021. Experimental evidence for hydrogen incorporation into Earth's core. Nat. Commun. 12 (1), 2588.
Terasaki, H., Kato, T., Urakawa, S., Funakoshi, K.-I., Suzuki, A., Okada, T., Maeda, M., Sato, J., Kubo, T., Kasai, S., 2001. The effect of temperature, pressure, and sulfur content on viscosity of the Fe–FeS melt. Earth Planet. Sci. Lett. 190 (1), 93–101.
Terasaki, H., Suzuki, A., Ohtani, E., Nishida, K., Sakamaki, T., Funakoshi, K., 2006. Effect of pressure on the viscosity of Fe-S and Fe-C liquids up to 16 GPa. Geophys. Res. Lett. 33 (22).
Umemoto, K., Hirose, K., 2015. Liquid iron-hydrogen alloys at outer core conditions by first-principles calculations. Geophys. Res. Lett. 42 (18), 7513–7520.
Urakawa, S., Terasaki, H., Funakoshi, K., Kato, T., Suzuki, A., 2001. Radiographic study on the viscosity of the Fe-FeS melts at the pressure of 5 to 7 GPa. Am. Mineral. 86 (4), 578–582.
Vočadlo, L., Alfè, D., Price, G.D., Gillan, M.J., 2000. First principles calculations on the diffusivity and viscosity of liquid Fe–S at experimentally accessible conditions. Phys. Earth Planet. Inter. 120 (1), 145–152.
Wang, W., Li, Y., Brodholt, J.P., Vočadlo, L., Walter, M.J., Wu, Z., 2021. Strong shear softening induced by superionic hydrogen in Earth's inner core. Earth Planet. Sci. Lett. 568, 117014.
Yeh, I.-C., Hummer, G., 2004. System-size dependence of diffusion coefficients and viscosities from molecular dynamics simulations with periodic boundary conditions. J. Phys. Chem. B 108 (40), 15873–15879.
Yuan, L., Steinle-Neumann, G., 2020. Strong sequestration of hydrogen into the earth's core during planetary differentiation. Geophys. Res. Lett. 47 (15), e2020GL088303.
Zhang, Y.-G., Guo, G.-J., 2000. Molecular dynamics calculation of the bulk viscosity of liquid iron–nickel alloy and the mechanisms for the bulk attenuation of seismic waves in the Earth's outer core. Phys. Earth Planet. Inter. 122 (3), 289–298.
Zhang, Y., Guo, G., Nie, G., 2000. A molecular dynamics study of bulk and shear viscosity of liquid iron using embedded-atom potential. Phys. Chem. Miner. 27 (3), 164–169.